International Journal of Enhanced Research in Science Technology & Engineering, ISSN: 2319-7463
Vol. 3 Issue 10, October-2014, pp: (102-112), Impact Factor: 1.252, Available online at: www.erpublications.com

Power Management and Control Strategy in Standalone DC Microgrid alongwith SMES Solenoid Coil

A. H. Moghadasi[1], A. Sundararajan[2], A. I. Sarwat[3]
[123]Electrical and Computer Engineering, Florida International University, Miami, USA

Abstract: This paper investigates the integration of Superconducting Magnetic Energy Storage (SMES) System into the standalone Permanent Magnet Synchronous Generator (PMSG) based on Variable Speed Wind turbine (VSWT) in DC Microgrid system. The primary aim of SMES system is to retain power balance by drawing power during high wind generation and to extricate it during low power generation. An effective control approach is produced for bi-directional DC-DC converter to balance the output power of the wind turbine depending on the load, consequently decreasing the capacity of the DC-DC converter system. To certify that the system can exploit under island conditions, a coordinated strategy for the SMES system, wind turbine and demands is proposed. Detailed simulation studies implemented in PSCAD/EMTDC emphasize the superior robustness of applying SMES coil in the DC Microgrid for damping down the wind power intermittency and for enhancing its dispatchability.

Keywords: DC Microgrid, Distributed Energy Resources (DER), Permanent Magnet Synchronous Generator (PMSG), Superconducting Magnetic Energy Storage (SMES), wind turbine.

Introduction

Recently, microgrids with Distributed Energy Resources (DER) and loads have been introduced to pose controversial for the future of electrical power systems [1], keeping in mind the results observed while tracking several outages and power disturbances that are caused by human error, poor maintenance and extreme weather events. End-user and DER entities are connected to each other via a DC bus (called DC-Link) in islanding mode of configurations such that the failure of one entity does not necessarily affect the other entities. This kind of an infrastructure is termed as a standalone DC Microgrid [2]-[4].

Furthermore, wind turbines with standalone mode of operation are becoming more prevalent. Such turbines have a crucial role in the sustainable energy development and implementation of a smart DC distribution system. A Permanent Magnet Synchronous Generator (PMSG), which has gathered special attentions in a standalone mode due to its simplicity, low maintenance requirements and high-efficiency operation, can enhance the stability of the Variable Speed Wind turbine (VSWT) [5-7]. Varying speeds of the wind causes intermittency in the power generation. Despite the inertia of the turbines, the overall output of the DC grid does not match the demand. This calls for the inclusion of additional energy storage devices to optimize and enrich the power system reliability and stability [8]. Obviously, charging and discharging efficiency is the major issue for storage devices used in power management.

Much of the research has already been done on the short-term response energy storage devices such as flywheels, super-capacitors and Superconducting Magnetic Energy Storage (SMES) system [9]. The characterization of these storage devices is illustrated in Table 1. Regulation of power fluctuations is vital to establish a reliable and stable grid. Energy storage devices work by injecting the deficit power and absorbing the power in excess, thus smoothing the effective load. SMES is a novel superconducting technology which has been observed to be not just reliable but also quite effective [10]-[13]. The most prominent characteristic of the SMES is its high power density which is 10 times higher than those of the lead acid battery and NaS battery [14]. SMES systems store energy in a magnetic field created by DC current flowing through a superconducting coil that has been cryogenically cooled. Recent advancements in the field of power electronics coupled with the birth of sophisticated cryogenic systems has instigated a swell of potential for using SMES as an effective Energy Storage System (ESS) [15], [16]. Over the last year, several researches have been documented on various operational modes and control strategies of VSWT-PMSG based DC microgrid along with ESS [17], [18]. Much work has been done on using batteries and fuel cells as the energy storage devices. More commonly, the batteries work with controllers in Hardware-in-the-loop mode. However, there has been little work associated with the use of SMES on the standalone DC Microgrid. This paper endeavors to fill this deficiency by rendering a combinatorial standalone VSWT-PMSG and SMES system in order to stabilize the dc-link voltage, thereby enhancing wind power dispatchability.

Table 1: Short-term response energy storage devices characterization [10], [11].

Characteristics	Technology		
	Flywheels	Super capacitors	SMES
Energy (MWh)	< 5	< 3	< 1000
Power (MW)	< 10	< 10	< 100
Efficiency	90 %	90 %	95 %
Life-time (cycles)	10^6	10^6	10^6
Price (€/kW)	140-350	70-400	200-500

To start, with careful consideration of wind deviations and practical restriction, the SMES coil is designated a precise energy storage capacity. Then, the real-time energy management strategy targeting the close coordination between the wind powers, loads, and SMES system in reference to power and current measurement is presented. For this purpose, the effective approach for bi-directional DC-DC converter is expounded resulting in an optimized charging and discharging model of the SMES system.

System Configuration and Modeling

A. System Layout

The proposed combination of the standalone DC Microgrid system is schematically shown in Fig. 1. In this topology, the original source of power generation is a wind turbine utilizing PMSG which is rated at 2100kW and 690 V. The generator-side converter, including the three-phase Voltage Source Converter (VSC) rated at 1 MW, namely, W-VSC, is used to connect the PMSG to the DC network. The Energy Storage (ES) system that is based on SMES technology is combined into the DC network through a bidirectional DC–DC converter as illustrated in Fig. 1. In order to increase the energy efficiency of the system, an effective dump load is used. It works by absorbing the excess power during an excessive wind generation and surplus energy is expended in charging the SMES until the current reaches its upper limit. After that, the extra power is supplied to a proper dump load for heating, with DC-DC converter. DC loads can be either direct-connected or sensitive in nature. It is ensured that the net power generated by the wind turbine is fed into the variable DC loads. To guarantee the system against a total collapse and cater to a secure power supply to high priority loads (sensitive loads), an appropriate load shedding must be considered during the prolonged operation in low-wind mode.

B. Maintaining the Integrity of the Specifications

The mechanical power output of wind turbine extracted from the wind power can be determined by mathematical relation as follows [19]

$$P_w = \frac{1}{2}\rho A^2 V_w^3 C_P(\lambda, \beta) \qquad (1)$$

where ρ is the air density [kg/m^3], A is the blade area [m^2], V_w is the wind speed [m/s] and C_p is the power coefficient which is a function of tip-speed ratio, λ, and the blade pitch angle, β [deg].

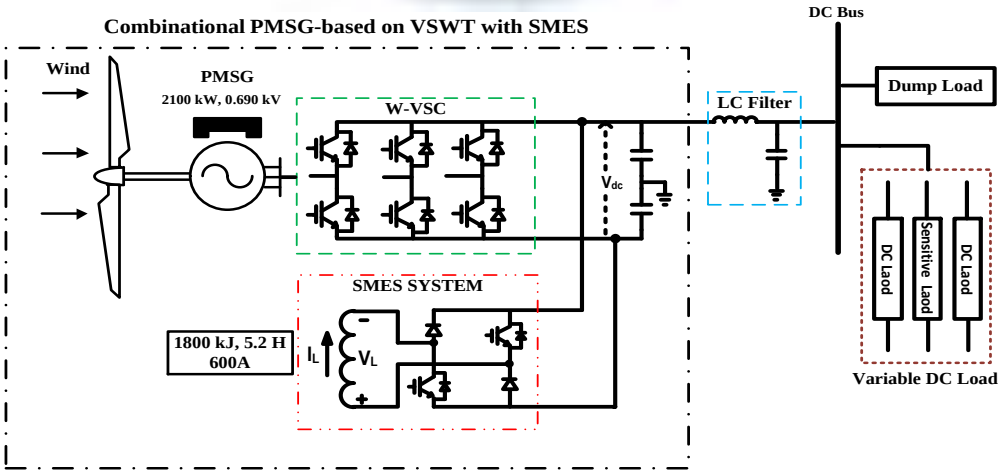

Figure 1. Combination of PMSG- based on VSWT and SMES system in dc microgrid.

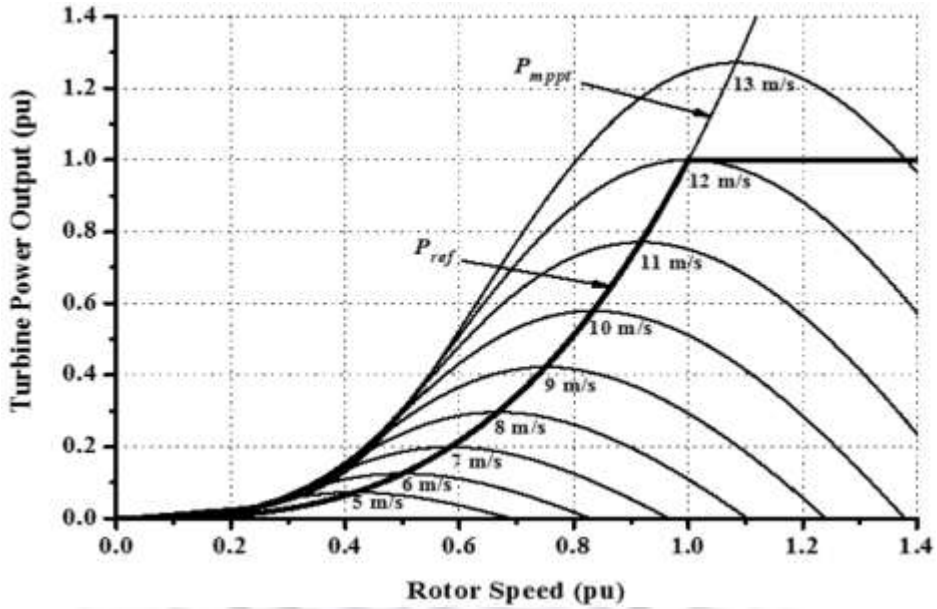

Figure 2. characteristic of Turbine power (β=0o) [20].

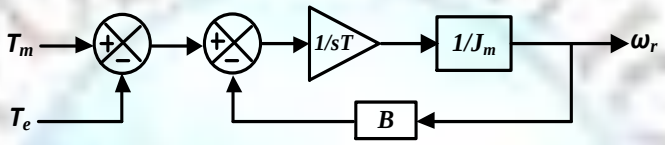

Figure 3. Modeling of wind turbine system drive-train.

In a variable speed PMSG-based wind turbine, the rotor speed (ω_r) is measured to achieve maximum power point tracking (MPPT). The maximum power (P_{max}) can be computed without extracting wind speed as given in (2). The reference power (P_{ref}) is restricted within the rated power of machine.

$$P_{\max} = \frac{1}{2}\rho A^2 \left(\frac{R\omega_r}{\lambda_{opt}}\right)^3 C_{P\text{-}opt} \qquad (2)$$

where λ_{opt} and $C_{p\text{-}opt}$ are the optimum values of the tip speed ratio and power coefficient, respectively.

Fig. 2 illustrates the relation between the rotor speed and output power of wind turbine for various wind speeds with the blade pitch angle $\beta=0^o$.For an average wind speed of 12 m/s, which is used in this paper, the maximum turbine power output and rotational speed are 1.0 p.u. Theone-mass model based on deriving the state equation is considered for the rotor angular speed to specify derive train of the wind turbine generator, represented by

$$J_m \frac{d\omega_r}{dt} = \left(T_m - T_e - B\omega_r\right) \qquad (3)$$

where J_m is the moment of inertia for the blades, hub and generator, T_m is the mechanical torque, T_e is the electric torque and B is rotational damping. The utilized block diagram for modeling of wind turbine system drive-train is shown in Fig. 3.

SMES System Description

In this effort, the SMES system is implemented as a promising ES system for load balancing and power stabilizing in standalone DC Microgrid. Generally speaking, an SMES system consists of a superconducting coil which stores energy in the magnetic field, cryogenic refrigerator to maintain coil at a low temperature so that it is maintained in superconducting state and a Power Conditioning System (PCS) in order to exchange the energy from the SMES coil into the grid. Although the balancing performance of SMES coil can be increased by selecting a larger capacity, however the cost installation of SMES system will increase accordingly, making the implementation of SMES unviable. In opposite, selecting an insufficient capacity for SMES system will most likely lead to an inconclusive operation for diminishing

wind power intermittences. Therefore, the coil capacity must be carefully chosen, bring in mind its application and charging/discharging duration. For a DC Microgrid which is equipped by VSWT-PMSG, if SMES balances the fluctuating power $\pm\Delta P_{wind}$ for a period of Δt seconds, the SMES requires to compensate $\pm\Delta P_{wind}\times\Delta t$ stored energy duo to the intermittent wind fluctuations. As stated in (1), the wind power is proportional to the third power of wind speed. If the standard deviations of wind speed fluctuations is 20% of the average wind speed [12], the output power fluctuations will be about 80% (ΔP_{wind} = 1680 kW for period of 1 second) of the rated 2100 kW from the wind power. Therefore, the capacity requirement of the SMES system can be estimated as following

$$E_{required} = \Delta P_{wind} \times \Delta t = 1680\ kW \times 1s = 1680 kJ \quad (4)$$

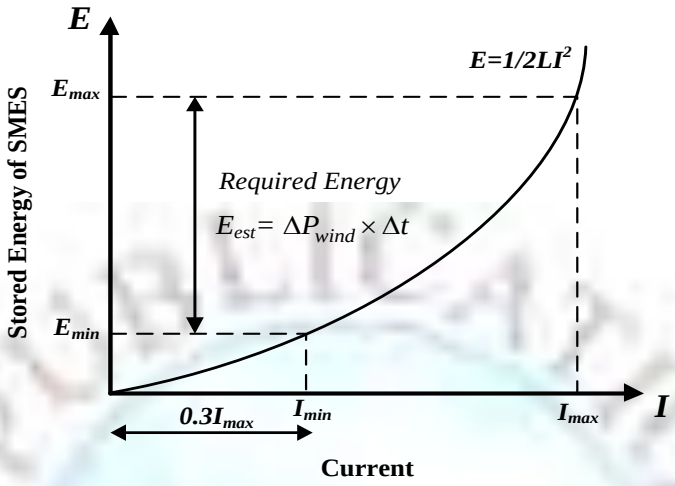

Figure 4. Estimated energy of the SMES according to lower and upper coil current limits (Adapted from [12]).

In practice, in order to prevent the possibility of discontinuous conduction under unexpected disturbances, SMES current, I_{smes}, is not allowed to reach zero [8]. Fig. 4 shows the relation between the stored energy of the SMES and the available energy for the wind turbine based on lower and upper coil current limits (I_{min} = $0.3I_{max}$<I_{smes}<I_{max}). Here, E_{max} can be calculated from (4) and Fig. 4 which has a relation best described as

$$E_{max} = \frac{E_{required}}{(1-0.3^2)} \cong 1800\ kJ \quad (5)$$

According to the above results, the maximum current flowing through the coil at an Inductance of 10 H can be obtained from the following equation.

$$I_{max} = \sqrt{\frac{2\times E_{max}}{L_{coil}}} = 600\ A \quad (6)$$

Control Scheme in Standalone Operation

The coordination control scheme utilized in DC Microgrid, including a W-VSC and DC–DC chopper, is presented in Fig. 6. The standalone operation mode requires that the common DC bus voltage should be maintained within an acceptable range which is usually 0.95 pu to 1.05 pu under any condition. Indeed, a constant DC voltage designates a balanced active power flow among the wind power, SMES system and DC loads.

A. VSC Converter Control

The control block diagram for a VSC converter shown in Fig. 5 is based on the synchronous d-q reference frame [21], [22]. A Maximum Power Point Tracking (MPPT) is used to estimate the active power reference, P_{max}, in a way explained before. Also, under regular operational conditions, the reactive power produced by the wind turbine is regulated at zero MVar (Qg_{ref} =0). In W-VSC converter, a triangle signal is used as the carrier wave for the PWM operation. The carrier frequency is chosen to be 10 kHz for the VSC converter with the result showing DC link capacitance to be 18000 µF and the rated DC-link voltage across the capacitor legs to be 800 V.

B. Bi-directional DC-DC Converter Control

A DC-DC bi-directional converter is used to interconnect the SMES and the DC link in order to facilitate the active power flow in both directions, as represented in Fig. 6. It is considered to be fully charged at around a maximum capacity of 880 kJ. The two IGBTs, S_A and S_B, are fired using hysteresis band current control technique [23]. The

control of the IGBTs is performed by the analogy of power generated by the wind turbine, P_{wind}, and the power consumed by the load, P_{load}. In order to keep system stability, the SMES system must be charged or discharged corresponding to the required power balancing as given by the following equation.

$$P^*_{smes} = P_{wind} - P_{load} \quad (7)$$

where superscript * represents the required (reference) value.

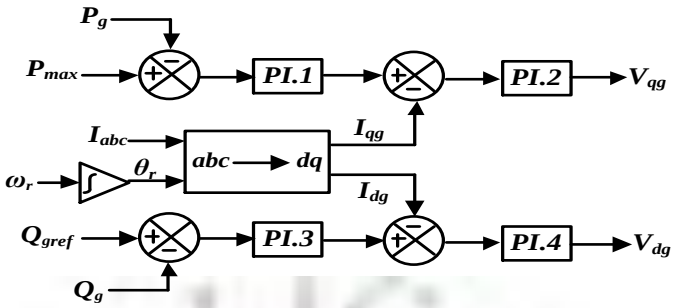

Figure 5. Generator side controller of PMSG.

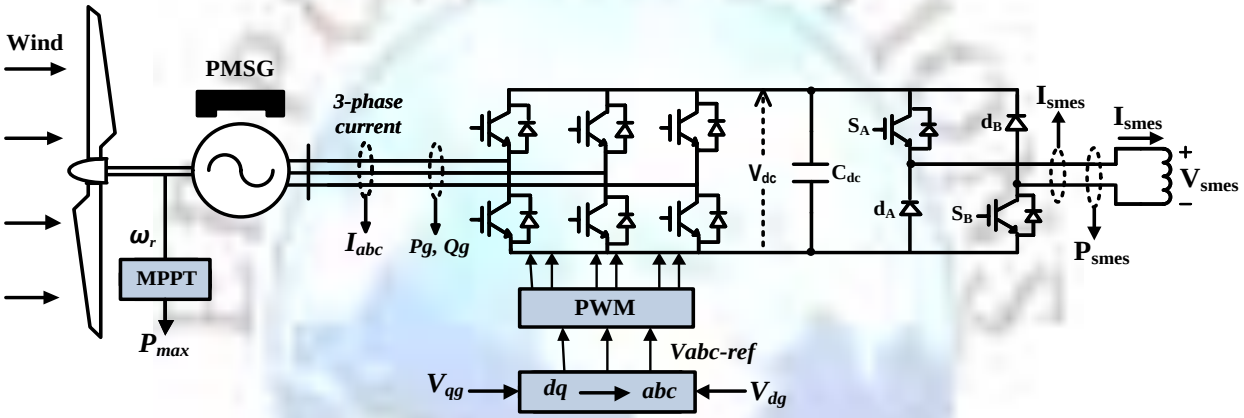

Figure 6. Control diagram of PMSG-based variable speed wind turbine

A DC Microgrid is assumed to be operating in an acceptable fashion during an erratic period of wind generation if three operational zones can be known for the DC-DC converter.

Standby mode: It occurs when the output power of the wind turbine is equivalent to the demand side power ($P^*_{smes}= 0$). With the SMES coil current fixed at its rated value, it is observed that there will be no energy exchange between the SMES system and DC Microgrid.

Discharging mode: It will take part when the output power of the wind turbine is smaller than the rated power ($P^*_{smes}< 0$). In this case, the required power will be output to the DC link capacitor with a DC-DC converter.

Charging mode: When the wind turbine generates power that surpasses the rated power ($P^*_{smes} > 0$), the converter happens to be in this mode, wherein the surplus power produced is relocated to the SMES coil. The following equation describes the SMES coil current, I_{smes1}, at the end of the exchanging period, T.

$$I_{smes,1} = \sqrt{I^2_{smes0} - \frac{2 \times \left(\int_T P^*_{smes} \right)}{L_{smes}}} \quad (8)$$

where E^*_{smes} is energy transfer between the SMES system and DC link (J), L_{smes} is the coil inductance (H) and I_{smes0} represents the coil current at the beginning of the exchanging period. In this paper, it is assumed that the superconducting coil is being charged or discharged based on an exponential function represented in the following equations

$$I_{discharge}^{ref} = I_{smes,0} \times e^{-\alpha(t-t_d)} \quad (9)$$

$$I_{charge}^{ref} = -I_{smes,1} \times e^{-\beta(t-t_d)} \quad (10)$$

$$\alpha = \beta = \frac{1}{T} \times Ln\left(\frac{I_{smes0}}{I_{smes1}}\right) \quad (11)$$

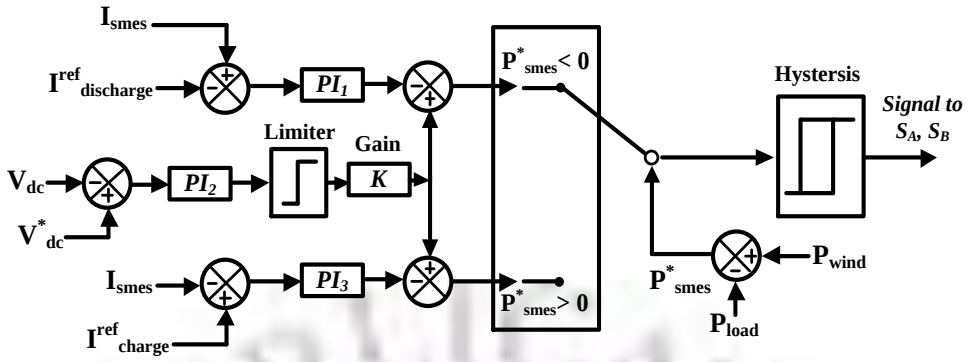

Figure 7. Control diagram of dc-dc converter with SMES coil.

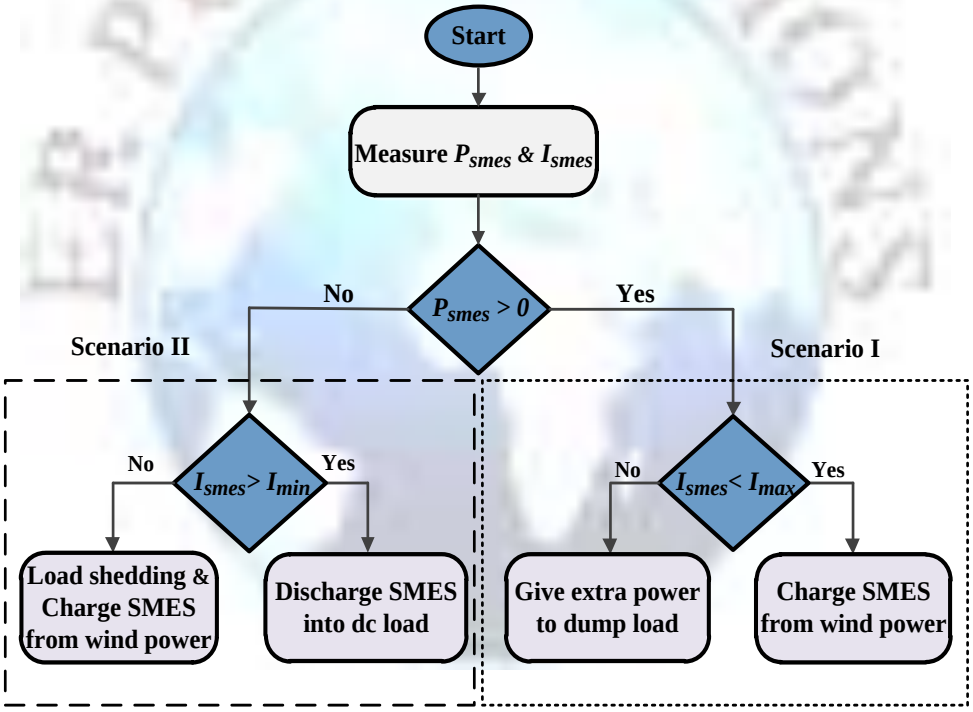

Figure 8. Energy management strategies for the standalone DC Microgrid.

Appropriate operation of the control system occurs when the coil current tracks these reference currents during the charging/discharging operation mode.

In order to produce the gate signals for the G_A and G_B, the reference duty cycle signals must be compared with the carrier by frequency of 4 kHz. A schematic representation of the DC–DC converter controller used to regulate the current of the SMES to maintain the DC bus voltage constant is depicted in Fig. 7.

C. Power Management Scheme

Particularly, during long-term low-wind or high-wind periods, an appropriate real-time power management must be implemented in place into the control system to optimize the energy utilization. It maintains the DC bus voltage constant. The flowchart for the suggested energy management algorithm, which accounts for two scenarios, is annotated in Fig. 8.

Scenario 1: The SMES coil can be charged with the excess power that results when the power available from the VSWT-PMSG exceeds the demand to the point when its current reaches the upper limit (I_{max}). While diverting the extra power to a proper dump load, the SMES is set to attain a standby mode. However, this condition is outside the scope of the study.

Scenario 2: When the power generated by the wind turbine does not meet the demand, the cumulative voltage of the DC Microgrid tends to collapse. In order to avoid this hazardous downfall, the SMES needs to be discharged. By taking into consideration the latest reduced demand, the SMES system is designed to toggle its control from discharging to charging mode in order to absorb the additional wind power. This happens when the non-sensitive load gets automatically disconnected as a result of the SMES coil current exceeding its lower limit of $0.4I_{max}$.

Numerical Simulation Results

This section elucidates the different simulation studies conducted with the aim of analyzing the effectiveness of the standalone DC Microgrid that uses PMSG-based wind turbine and SMES system, as depicted by Fig.1. Moreover, the evaluation method discussed in this section augments the system efficiency of the DC Microgrid by using different criteria like cost-efficiency, energy saving and economizing as the primary vantage points.

A. Case Studies

Modeling and simulation of the proposed system is done on PSCAD/EMTDC. The system, as portrayed by Fig. 1, comprises the PMSG-based wind turbine that is rated at 2100kW W-VSC possessing a switching frequency of 10 kHz. L_1 and L_2 are rated at a constant power load value of 330 kW with L_1 being an indispensable component during the operation.

Table 2: Main Operation Events for Case 1

Events	Operation condition	Time (s)
1	SMES starts to discharging	10
2	SMES capacity reaches 0.55 pu	11.5
3	SMES starts to charging	14
4	SMES capacity reaches 0.95 pu	16

Fig. 2 demonstrates the observation that a wind turbine with a power rating of 2100 kW delivers sufficient power to the loads provided there is a driving wind speed of 12 m/s. A superconducting coil of 1800 kJ capacity and a bi-directional DC-DC converter form the SMES system. This system is connected to an 800 V bus through the DC-link capacitor. For the proposed SMES to operate in a proper fashion, two possible cases are analyzed below:

Case 1: Normal Charging/Discharging Operation

Normal charging/discharging operation of the SMES is illustrated in Fig. 9 while Table 2 enlists the prime operation events. The power of the wind turbine is equivalent to the overall load, as observed in Fig. 9(c), when, as projected by Fig. 9(a) and Fig. 9(c) respectively, L_1 (1600 kW) and L_2 (500 kW) are switched as total P_{load} = 2100 kW and the torque reference reduced to 0.63pu owing to an initial wind speed of 12 m/s. Under such circumstances, the SMES coil charges to its maximum current of 600 A.

Event 1: Consider the case where the wind speed dips to 10 m/s at 10s. As a consequence, the power from the wind turbine drops to 1400 kW that happens to be less than the demand. The SMES system is hence expected to supply the balance power of 700 kW in order to attain an equilibrium state with a constant load of 2100 kW (discharging mode). Fig. 9(b) throws light on the fact that the SMES current is decreased to about 390 A as a result of the discharging mode the system is in.

Event 2: In this stage, the speed of the wind returns to 12 m/s, at around 11.5 s, but the SMES neither draws nor supplies power to the DC Microgrid since its current remains in the standby mode.

Event 3, 4: When the wind speed increase by 13 m/s at 14 s and eventually attains the generated power of 2500 kW, an excess power of 400 kW must be pulled by the SMES system to maintain the DC voltage at less than 1.05 pu. Fig. 9(c) pictorially represents this observation. Current in the coil shoots from 390 A to 585 A, triggered by this state of the system, and as a result, the SMES capacity is set back to a value around its maximum. It can be concluded that the performance of the proposed control method is conveniently acceptable, considering the fact that, as exhibited by Fig.

9(b), the charging and discharging currents follow the reference currents in a favorable manner. SMES is also observed to curb the output DC-link voltage at a constant load, as represented in Fig. 9(e).

Case 2: Long-Term Low-Wind Operation

Fig. 10 and Table 3 respectively demonstrate the simulation results of the system control and operations that are pertinent to Case 2, and the list of main operation events. It is assumed that the state of the system before simulation is the same as the one before simulation for Case 1.

Event 1: Commencing at 10 s, the wind speed deteriorates by a unit from 11 m/s for a period of 4 s. SMES upsurges its power output to recompense the imbalance interjected and hence maintain the DC-link voltage at 0.97 pu. This event is clearly exemplified by Figs. 10(a) and 10(d).

Event 2: At about 13 s, the SMES current is diminished to 240 A, that also happens to be equal to the threshold value (0.4Imax). The system is engineered to spare energy for the most imperative load, L_1 in this instance. This prompts the tripping of L_2 at 500 kW, initiating the charging of the SMES as observed from Fig. 10(b) because the wind turbine spawns more power than the current reduced demand (L_1).

Event 3: The wind speed now increases to 13 m/s at 14 s, after supportingL_1 for a second. The SMES gradually gets charged as a consequence to about 2400 kW. L_2 gets reconnected to the microgrid, as can be seen from Fig. 10(c). By the end of this period, the coil current attains a value of 480 A, as can be referred to from Fig. 10(b).

Event 4, 5: Lastly, when the wind speed decreases to 11.5 m/s, the power from the wind turbine shrinks to 1800 kW that is less than the demand. This necessitates an injection of 300 kW power by the SMES. Figs. 10(e) reveal the satisfactory performance of the proposed control strategy owing to efficient control of the dynamic trait of the wind and the DC-link voltage during numerous operating conditions. Employing an exponential function, this ubiquitous technique finds optimal charging and discharging models.

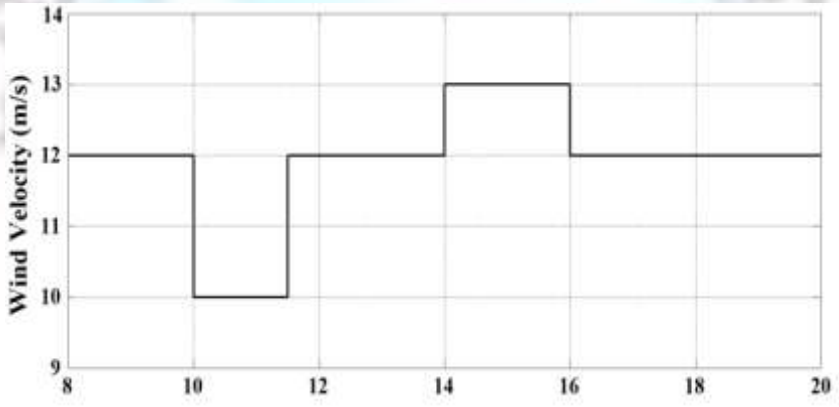

(a)

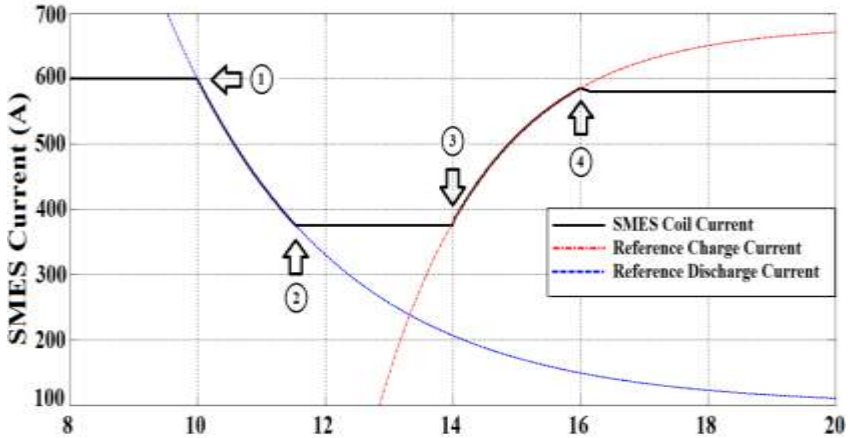

(b)

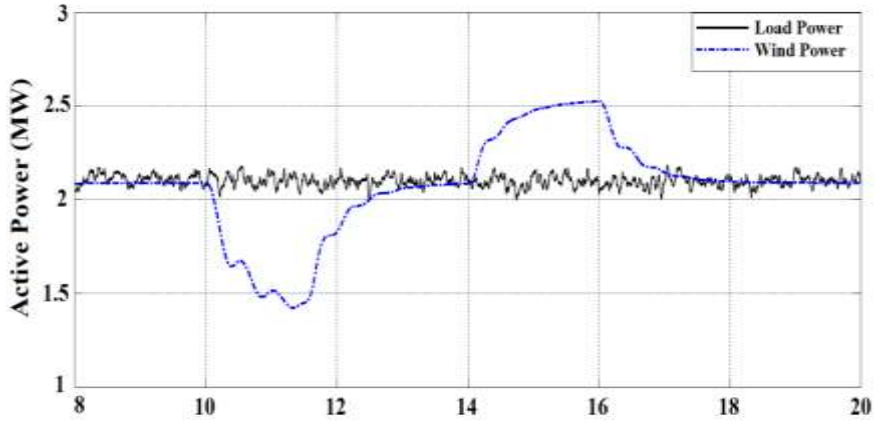

(c)

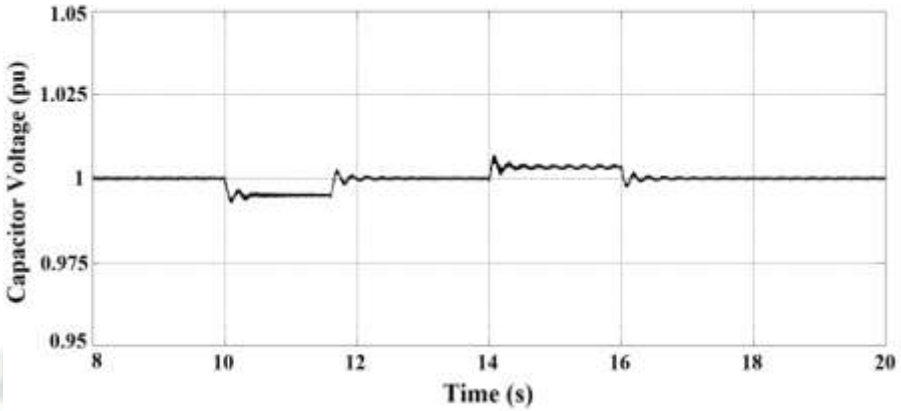

(d)

Figure 9. **System operation during normal charging/discharging mode (Case 1). (a) Wind speed. (b) SMES coil current. (c) Power generated by the wind turbine and total load. (d) DC-link voltage.**

Table 3. Main Operation Events for Case 2

Events	Operation condition	Time (s)
1	SMES starts to discharge	10
2	L_2 switched out and SMES start to charge	12.5
3	L_2 switched in and SMES starts to charge	14
4	SMES capacity reaches 0.73 pu	16
5	SMES starts to discharge	18

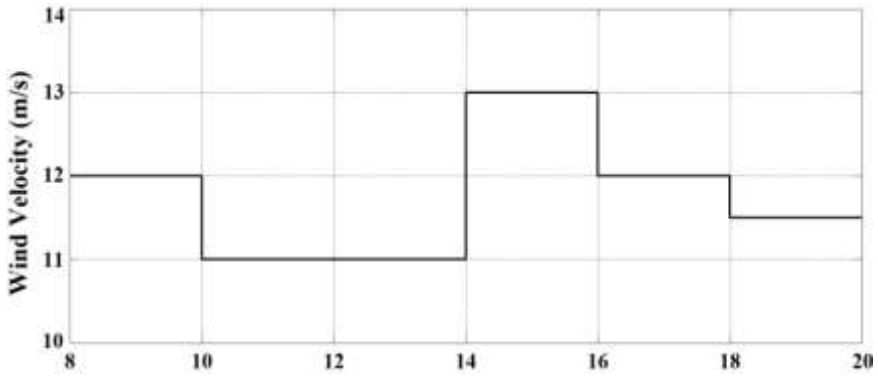

(a)

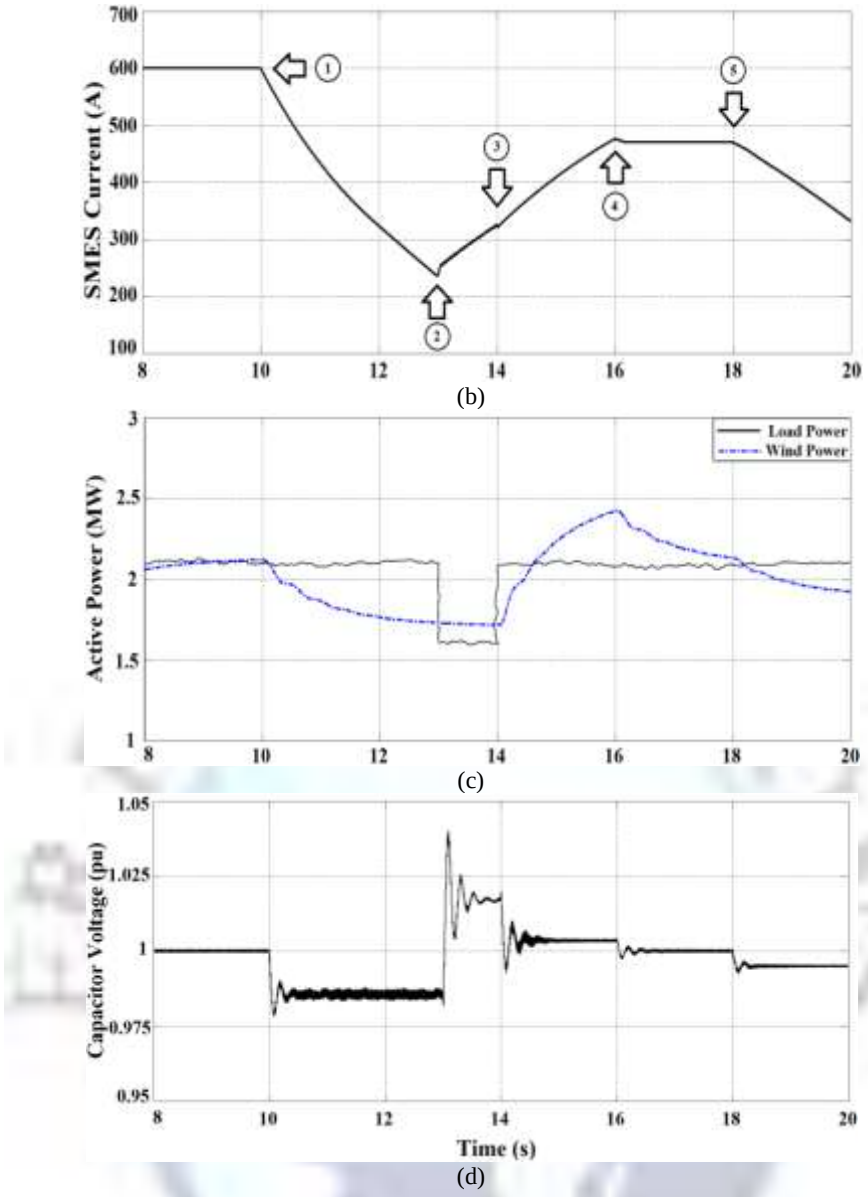

Figure 10. **System operation during prolonged low-wind mode (Case 2). (a) Wind speed. (b) SMES coil current. (c) Power generated by the wind turbine and total load. (d) DC-link voltage.**

Conclusion

This work has accomplished a detailed study on the SMES system integrated into the VSWT-PMSG by interconnecting it to the standalone DC Microgrid through a bi-directional DC-DC converter. The potential of supervisory control architecture is exploited to address the issue of maintaining the power balance between the SMES and the intermittent power generation characteristics of the wind. Steadying the DC-link voltage forms the focal point of the paper. An efficient controller model to empower the SMES against the rapid vacillations in the wind power is proposed. An added merit of this strategy is the simultaneous smoothening of the output power. Further research can focus on honing the physiognomies and operations of the SMES system by imbibing more practical elements such as cost-appraisal of the SMES system, a widespread scrutiny of the wind speed discrepancies and the readiness factor of the wind power system when perceived as a single entity.

References

[1]. Guerrero, J.M.; Blaabjerg, F.; Zhelev, T.; Hemmes, K.; Monmasson, E.; Jemei, S.; Comech, M.P.; Granadino, R.; Frau, J.I., "Distributed Generation: Toward a New Energy Paradigm," Industrial Electronics Magazine, IEEE , vol.4, no.1, pp.52,64, March 2010.

[2]. N. Hatziargyriou, H. Asano, R. Iravani, and C. Marnay, "Microgrids," IEEE Power Energy Mag., vol. 5, no. 4, pp. 78–94, Jul./Aug. 2007.

[3]. T. Senjyu, T. Nakaji, K. Uezato, and T. Funabashi, "A hybrid power system using alternative energy facilities in isolated island," IEEE Trans. Energy Convers., vol. 20, no. 2, pp. 406–414, Jun. 2005.
[4]. Akbari, M.; Tafreshi, S. M M; Golkar, M.A., "Voltage control of a hybrid ac/DC Microgrid in stand-alone operation mode," Innovative Smart Grid Technologies - India (ISGT India), 2011 IEEE PES , vol., no., pp.363,367, 1-3 Dec. 2011.
[5]. Bhende, C.N.; Mishra, S.; Malla, S.G., "Permanent Magnet Synchronous Generator-Based Standalone Wind Energy Supply System," Sustainable Energy, IEEE Transactions on , vol.2, no.4, pp.361,373, Oct. 2011.
[6]. Moghadasi, Amir; Islam, Arif, "Enhancing LVRT capability of FSIG wind turbine using current source UPQC based on resistive SFCL," T&D Conference and Exposition, 2014 IEEE PES , vol., no., pp.1,5, 14-17 April 2014.
[7]. Lie Xu; Dong Chen, "Control and Operation of a DC Microgrid with Variable Generation and Energy Storage," Power Delivery, IEEE Transactions on, vol.26, no.4, pp.2513, 2522, Oct. 2011.
[8]. Ngamroo, I., "Simultaneous Optimization of SMES Coil Size and Control Parameters for Robust Power System Stabilization," Applied Superconductivity, IEEE Transactions on, vol.21, no.3, pp.1358, 1361, June 2011.
[9]. Moghadasi, A.H.; Heydari, H.; Farhadi, M., "Pareto Optimality for the Design of SMES Solenoid Coils Verified by Magnetic Field Analysis," Applied Superconductivity, IEEE Transactions on , vol.21, no.1, pp.13,20, Feb. 2011.
[10]. Toshiyuki Mito, "Development of UPS-SMES as a Protection from Momentary Voltage Drop", IEEE Transactions on Applied Superconductivity, Vol. 14, N0. 2, pp 721-726, June 2004.
[11]. T. Sels, C. Dragu, T. Van Craenenbroeck, R. Belmans, "Overview of new energy storage systems for an improved power quality and load managing on distribution level", 16th International Conference and Exhibition on Electricity Distribution, Vol.4, pp 5, Amsterdam, June 2001.
[12]. R., "Wind farms linked by SMES systems," Applied Superconductivity, IEEE Transactions on, vol.15, no.2, pp.1951,1954, June 2005.
[13]. Moghadasi, A.; Torabi, S.M.; Salehifar, M., "Combined operation of the unified power quality conditioner with SFCL and SMES," Power Quality Conference (PQC), 2010 First, vol., no., pp.1,7, 14-15 Sept. 2010.
[14]. Taesik Nam; Jae Woong Shim; Kyeon Hur, "The Beneficial Role of SMES Coil in DC Lines as an Energy Buffer for Integrating Large Scale Wind Power," Applied Superconductivity, IEEE Transactions on, vol.22, no.3, pp.5701404,5701404, June 2012.
[15]. Yunus, A.M.S.; Masoum, M. A S; Abu-Siada, A., "Application of SMES to Enhance the Dynamic Performance of DFIG during Voltage Sag and Swell," Applied Superconductivity, IEEE Transactions on, vol.22, no.4, pp.5702009, 5702009, Aug. 2012.
[16]. J. Kondoh, I. Ishii, H. Yamaguchi, A. Murata, K. Otani, K. Sakuta, N. Higuchi, S. Sekine, andM. Kamimoto, "Electrical energy storage systems for energy networks," Energy Convers.Manag., vol. 41, no. 17, pp. 1863–1874, Nov. 2000.
[17]. H. Kakigano, Y. Miura, and T. Ise, "Low-voltage bipolar-type DC Microgrid for super high quality distribution," IEEE Trans. Power Electron., Vol. 25, No. 12, pp. 3066-3075, Dec. 2010.
[18]. A. Kwasinski and C. N. Onwuchekwa, "Dynamic behavior and stabilization of DC Microgrids with instantaneous constant-power loads," IEEE Trans. Power Electron., Vol. 26, No. 3, pp. 822-834, Mar. 2011.
[19]. Lin Ye; Liang Zhen Lin, "Study of Superconducting Fault Current Limiters for System Integration of Wind Farms," Applied Superconductivity, IEEE Transactions on, vol.20, no.3, pp.1233, 1237, June 2010.
[20]. Marwan Rosyadi, S. M. Muyeen, Rion Takahashi and Junji Tamura, "A Design Fuzzy Logic Controller for a Permanent Magnet Wind Generator to Enhance the Dynamic Stability of Wind Farms", Applied. Sciences.Vol.2, Issue 4, 2012.
[21]. Amir Hasan Moghadasi; Heydari, H.; Salehifar, M., "Reduction in VA rating of the Unified Power Quality Conditioner with superconducting fault current limiters," Power Electronic & Drive Systems & Technologies Conference (PEDSTC), 2010 1st , vol., no., pp.382,387, 17-18 Feb. 2010.
[22]. Heydari, H.; Moghadasi, A.H., "Optimization Scheme in Combinatorial UPQC and SFCL Using Normalized Simulated Annealing," Power Delivery, IEEE Transactions on , vol.26, no.3, pp.1489,1498, July 2011.
[23]. Bose, B.K., "An adaptive hysteresis-band current control technique of a voltage-fed PWM inverter for machine drive system," Industrial Electronics, IEEE Transactions on, vol.37, no.5, pp.402, 408, Oct 1990.